

We are IntechOpen, the world's leading publisher of Open Access books Built by scientists, for scientists

6,900

Open access books available

185,000

International authors and editors

200M

Downloads

Our authors are among the

154

Countries delivered to

TOP 1%

most cited scientists

12.2%

Contributors from top 500 universities



WEB OF SCIENCE™

Selection of our books indexed in the Book Citation Index
in Web of Science™ Core Collection (BKCI)

Interested in publishing with us?
Contact book.department@intechopen.com

Numbers displayed above are based on latest data collected.
For more information visit www.intechopen.com



Remotely Sensed Data for Assessment of Land Degradation Aspects, Emphases on Egyptian Case Studies

Abd-alla Gad

Abstract

Remote sensing and thematic data were used to provide comprehensive views of surface conditions related to land degradation and desertification, considered environmental extremes in arid and semi-arid regions. The current work applies techniques, starting with simple visual analyses up to a parametric methodology, adopted from the FAO/UNEP and UNESCO provisional methodology for assessment and mapping of soil degradation. Egyptian case studies are highlighted to insinuate on studied aspects. Variable satellite imageries (MSS, TM, and ETM) and aerial photographs were utilized to provide data on soil conditions, land cover, and land use. IDRISI and ArcGIS software were used to manage thematic data, while ERDAS IMAGIN was used to process satellite data and to derive the normalized difference vegetation index (NDVI) values. A GIS model was established to modify the universal soil loss equation (USLE) calculating the present state and risk of soil degradation. The study area is found exposed to slight hazard of water erosion, however, and to high risk of wind erosion. It is also threatened by a slight to high salinization and slight to moderate physical degradation. It is recommended to use a GIS in detailed and very detailed studies for evaluating soil potentiality in agricultural expansion areas.

Keywords: soil degradation, desertification, extreme environment, arid, remote sensing, GIS, Egypt, Sinai

1. Introduction

An extreme environment is a habitat characterized by harsh environmental conditions, beyond the optimal range for the development of humans [1]. For an area to be considered an extreme environment, it must contain certain conditions and aspects that are considered very hard for other life forms to survive.

It was recently realized [2] that numerous political decisions linked with land degradation and desertification research findings were promoted. Examples of such support are referred to the sustainable development call, issued at the UN Conference on Environment and Development. Also, the threat recognition to human welfare through processes of desertification represents that support expressed in

the United Nations Convention to Combat Desertification [3]. In this context, it has also been emphasized that research should support policy makers and administrative authorities dedicated to establishing locally adapted schemes for sustainable land management.

Although the methods for large scale land degradation assessments are commonly employed and well developed, a monitoring of land degradation and desertification processes, at more detailed, spatial and temporal scales using remote sensing data, is still an issue. This problem is documented in numerous publications discussing the severity of the space images that offer a synoptic view, multispectral and multi-temporal possibilities, and are nearly orthogonal. The synoptic view is possible because about 3.5 million hectares (8.6 million acres) of the earth's surface can be examined on each scene, and all the objects can be compared across the entire scene [4]. The multispectral capability of the satellite images allows the establishment of unique spectral signatures for vegetation and soil related objects. The temporal capability permits the soil test of soils, vegetation, and atmosphere at intervals of different periods (i.e., 18 days for the Landsat images and 1 day for the Meteosat). Due to the very high sensing altitude, the metric distortions of the image are very small. It is thus possible to use the same scale of the map and via superposition of images, with only minor differences.

Exploiting the information provided by remote sensing, it is essential to consider that, it is mandatory to provide stakeholders with an attractive scheme assessing present resources and, if possible, the temporal progress thereof. This objective cannot be met by conventional approaches alone, which commonly rely on field based mapping of ecological parameters, providing a high level of details but only limited spatial coverage. Further information is needed for larger landscape units (e.g., through integrating field-based approaches with remote sensing techniques). Methodologies based on remote sensing data make use of the synoptic advantage, repetitive coverage, and consistent perspective over large areas. Combined with the functionality of today's GIS generation, a powerful tool is provided for monitoring and assessing areas under the threat of the extremes, as land degradation and desertification.

2. Basic theories of land degradation and desertification monitoring

A weakness of many approaches analyzing land degradation and desertification processes is the lack of an intangible outline, defining the reasons for undertaking monitoring in a certain way and how related difficulties could be faced. The necessary outline is not only restricted on accurate description of the respective threats but also a definition of the suitable methodology to face these challenges [5]. On the one hand, remote sensing data play an important role as one of the major sources of up-to-date and physically based information. On the other hand, GIS delivers the toolbox that enables data integration, analysis, and information extraction.

2.1 Processes, indicators, and scale

In order to understand how remote sensing and GIS may support the evaluation of land degradation/desertification threats for different ecosystems, it is needed to understand the environmental setting of these systems. Only a precise knowledge about governing processes leads to monitoring options and to develop meaningful conclusions on how to combat the respective threats. There have been numerous

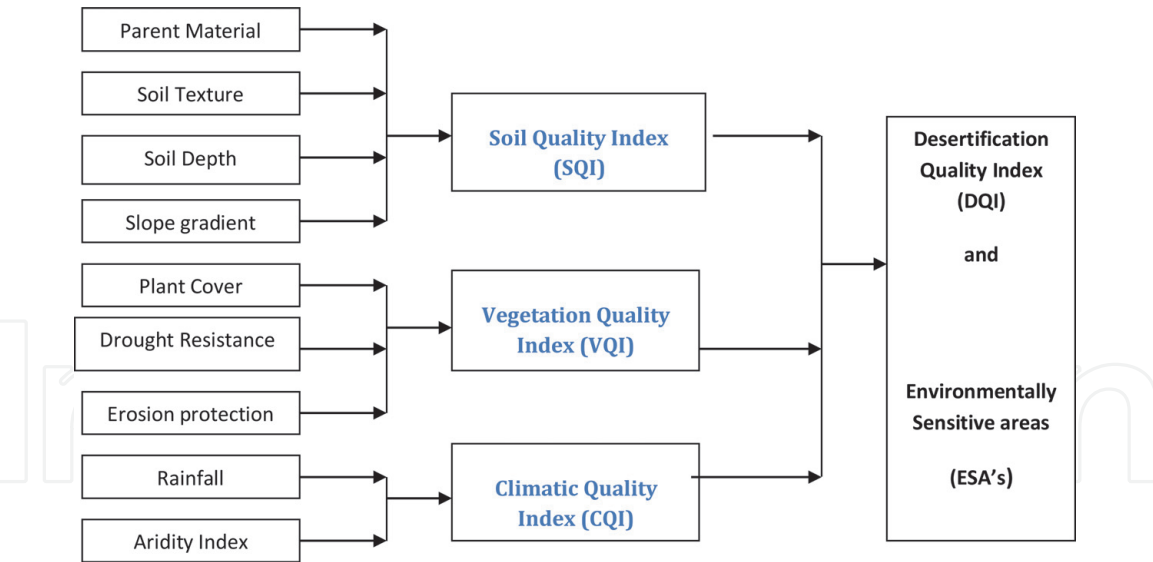


Figure 1.
Flow chart of mapping environmentally sensitive areas (ESAs).

approaches to conceptualize a chain from triggering processes to potential effects. In the current chapter, both visual analyses and digital image processing develop a concept on how to derive useful indicators for land degradation/desertification monitoring on the basis of examples from the European Mediterranean.

2.2 Land degradation/desertification assessment methodologies

A first and simple operated approach may concentrate on geological/geomorphological, climatic, and anthropogenic factors and their interrelationships. This basic approach has been expressed in the assessment of the present status, rate, and risk of land degradation processes [6]. It is included in EU funded DISMED project for assessment and mapping environmentally sensitive areas—**Figure 1**. Land degradation and desertification risk assessment depend upon factors determining changes in soil or vegetation properties. While we have to understand the logical chain of determinants, we have also to derive pathways on how to conclude from those processes on relevant indicators.

3. Environmental extremes in Egypt

3.1 General

Depending on the extreme physicochemical conditions that characterize the extreme environments, they are classified as *extreme temperature*: extremely cold environments and extremely hot environments, *extreme pH*: extreme acidic and extreme alkaline environments and *extreme pressure* environments are those under extreme hydrostatic or lithic pressure, such as aquatic habitats at depths of 2000 m or more or deep-subsurface ecosystems [1].

A region is arid when it is characterized by a severe lack of available water, to the extent of hindering or preventing the growth and development of plant and animal life [7]. Environments subject to arid climates tend to lack vegetation and are called xeric or desert. As located in the arid region, over two-thirds of Egypt is covered by the Western Desert. The desert is always dry, but it is actually not

lacking in water. Occasional rains fill huge underground aquifers beneath the desert, which occasionally break through to the surface. Just like along the Nile, water is the key to life here and where the water break through the surface thriving oases have formed around the springs. These isolated gardens in the desert have long supported substantial communities of people and substantial agricultural development as well as a culture unique from that of the Nile Valley.

3.2 Assessment of wind and fluvial action

Wind and fluvial actions have been fighting a wining battle against the small strip of the fertile Nile Valley. Historically, the western desert was a grave of Cambyses, king of Persia (50,000 soldiers) when he tried to attack the Siwa oases, Egypt (**Figure 2** shows the oases geographic distribution). The history also recorded about the lost oases in Wadi Hens, between Baharia oases north and Farafra oases in the south. These oases were covered by Eolian deposits. On the western side of the Nile Valley, the agricultural land in oases and depressions (**Figure 3**) is most suffering from the wind action. At the Kharga oases, dunes submerge roads and houses and encroach upon fields and whole villages. A complete village “Ginah” has been engulfed by sand in 1971. The government had built a new Ginah at short distance away to resettle farmers, however, is threatened now by other dune belts.

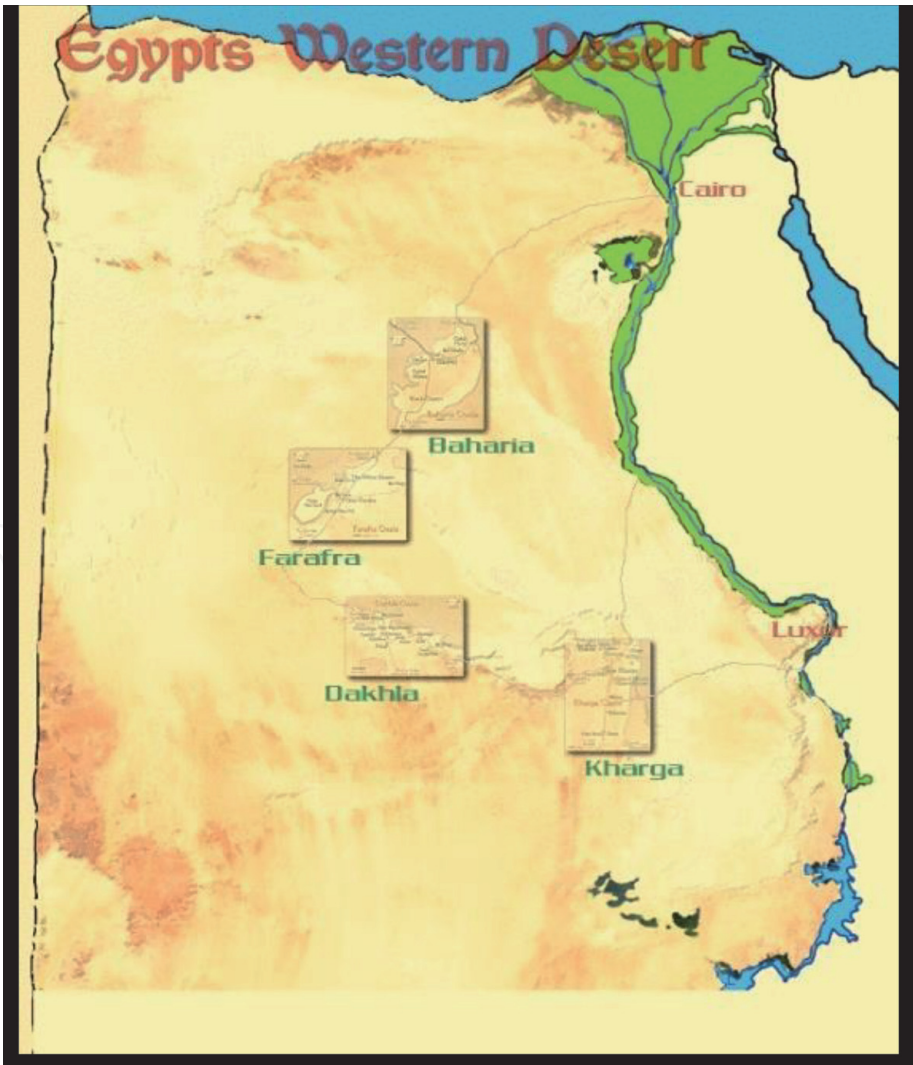


Figure 2.
Geographic distribution of western desert oases, Egypt.

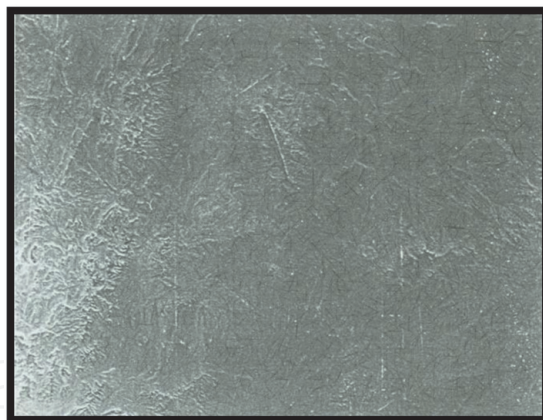


Figure 3.
Eolian deposits were blowing away, leaving deflation residuals in depressions, Egypt.

Despite the fact that methods for large scale degradation/desertification assessments are widely employed and well developed, however, monitoring at appropriate spatial and temporal scales and with adequate remote sensing methodologies is still uncommon. This problem is well documented in numerous publications discussing the severity of land degradation/desertification impacts from regional to global scale (e.g., [8–11]). Accordingly, impact assessments, of land degradation and desertification necessitate a thorough quantification of indicators in the context of global change research, as these processes inherently feedback into the integral development of global economy [7].

On the other side of the valley, the agricultural land is most suffering from the fluvial action. The heavy rainfall during thunderstorms causes severe erosion, threatening the cultivated land. The Menia Governorates has been exposed to strong destructive thunderstorms in the period between 1965 and 1975. The great amounts of the flooding water with their great power and suspended material have caused great physical damages in many villages with the consequent social extreme results. Also, a great thunderstorm has caused a great damage in the Qena area on April 13, 1985. One of the famous torrential extremes is one fallen over Nowaiba, on Red Sea coast in 1988, causing hundreds of deaths and great damages.

The current study aims to highlight the role of remote sensing techniques in assessment of wind and fluvial actions.

3.3 Detection of wind action

A simple visual interpretation of a false color composites (FCCs) of an ETM Landsat mosaic of 2014, covering Egyptian territories for bands 1, 2, and 3 rendered, respectively, in yellow, cyan, and magenta, was used. The images are enhanced photographically to get a maximum contrast in the desert area (**Figure 4**). The images revealed the Eolian deposits in the western desert in bright colors with some inclusion of dark patches. The rock land appears in dark colors mixed in some places with patches of bright ones indicating the existence of Eolian deposits and the rock land appear in different shapes according to their nature.

The satellite images show sand sheets located at the west of Nile Delta and along the western borders of the Nile Valley. The image is characterized by alternating light and dark streaks. The field investigation showed that these areas are covered by extensive sand sheets on an undulating land scape. Some areas were found to be



The image is used for delineation of different physiographic units ;

- 1) Undulating landscape "Teraces".
- 2) undulating landscape "Fan system"
- 3) Wadi bottoms
- 4) Windblown soils
- 5) Rock land
- 6) Denuded rock land
- 7) Alluvial Nile plain
- 8) Water body

Figure 4.
Color composite of ETM (2014) bands 1, 2, and 3 rendered, respectively, in yellow, cyan, and magenta.

covered by gravel and pebbles rather than by sand. It was found that the deposits are characterized by the alternation of layers (1–2 cm) of medium to fine sand and gravel. The image in the FCCs can be interpreted as, whereas light streaks are visible, as areas of deposition of fine-sized material (sand), the dark streaks are areas of non-deposition, erosion or bedrock surfaces.

3.4 Sand dune belts

These Eolian features can be observed developed out of denude able rock and at the south of the Faiyum Depression and extend in an elongated belt parallels to the Nile Valley. They are characterized by light colors, in the shape of parallel strips, alternating with dark colored strips in the same shape (**Figure 5**). The enlargement of Landsat band 3, to scale of 1:100,000 (**Figure 6**) reveals the individual existence of longitudinal dunes, inter-dune areas, and barchans dunes. The density of the longitudinal dunes differs: denser in the south of the Faiyum Depression while it is less dense in the west of the Menia. This variation in dune density is attributed to topographic effects, where scarps exist and increase in height, and they form a barrier to the prevailing winds that may enhance the relative effectiveness of winds from other directions. The longitudinal dune orientation indicates that the main wind direction is N-NW to S-SE.

Barchanoid dunes appear in the same Landsat ETM, as linear ones attaining barchans shaped ridges. Individual barchans, appearing in bright colored rounded and crescentic shaped patches are generated during extreme sand storm events.



Figure 5.
ETM (2014) Eolian features developed out of denude able rock south of the Faiyum Depression and extend in an elongated belt parallels to the Nile Valley.

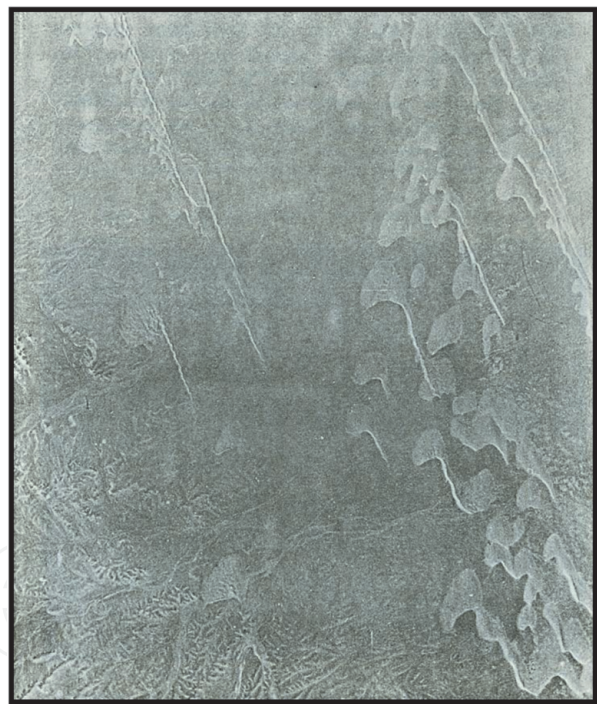


Figure 6.
The enlargement of Landsat 7, band 3, 2014 to scale of 1:100,000 reveals the individual existence of longitudinal dunes, inter-dune areas, and barchans dunes.

They exist in the leeward of some individual dunes. Some barchans dunes are large enough to indicate a general north-south direction with some deviations, having a west-east direction. Between the sand dunes, dark streaks occur in straight parallel orientation. These are indicating the gravelly corridors of the inter-dune areas, including faint appearing hydrographic network extending from the denuded rocky plateau to the accumulation areas of the debris material in the dune field, as a result of torrential action and the occasional thunder storms. These deposits are reworked by the wind during the long dry periods.

3.5 Erosional patterns

The synoptic view of Landsat images allows to see the rocky obstructs and their influence on the distribution of windblown sands. Isolated hills are also visible as obstacles to the wind transported sand. The rocky terrain appears on the FCCs in dark colors. Different color shades are attributed to importance of water bedrock outcrops and to the degree of erosion. Dark colors exist combined with light colors of the Eolian deposits. These are attributed to the denuded rock land, upon which windblown sands are deposited.

3.6 Detection of fluvial

The fluvial action is most clear in the eastern desert. It is possible to follow (Figure 7) the dense dendritic network of the wadis and ravines, which both are characterized by light colors, fine image texture, and dendritic pattern. These fluvial land forms are situated in the high plateaus. Areas of debris accumulation are distinct by their light color patches, which are situated adjacent to the east of the Nile Valley (Figure 8). Also, wide wadis are indicating the existence of debris material. In the wadi bottoms, huge amounts of material are deposited. The deposits are reflected in light colors controlled by wadi configuration. Wadi El-Bustan in the south of the eastern desert is a typical example. Most probably, the pattern of different wadis and tributaries was controlled by the area of weakness, and the run-off water of thunderstorms will follow these weak zones. The debris material endangers the eastern cultivated strip of the Nile Valley.

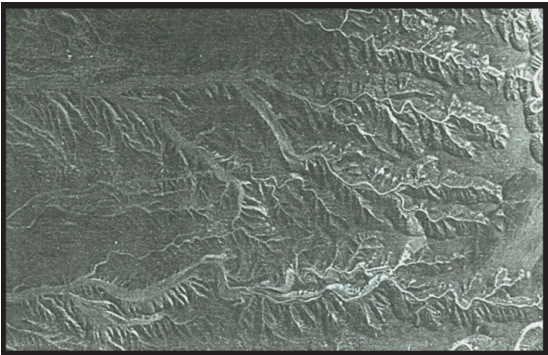


Figure 7.
Landsat ETM7—band 2 (2014) scale of 1:100,000 reveals fluvial degradation land forms at the Easter desert, Egypt, including dendritic drainages, ravines, and gullies.

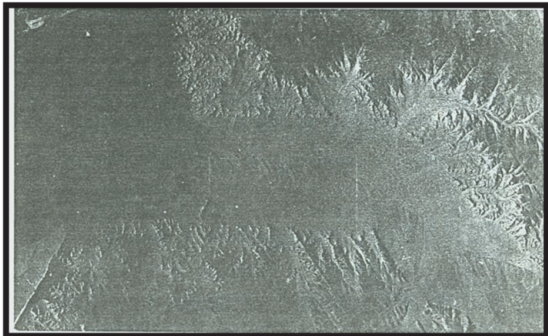


Figure 8.
Landsat ETM7—band 3 (2014) scale of 1:100,000 reveals fluvial depositional land forms at the Easter desert, Egypt, including alluvial fans.

4. Using Meteosat in the study of a thunderstorm on the eastern desert, Egypt

Meteosat sensors have been used for many meteorological applications [12, 13]. It was used for example in wind vector determination [14]. Meteosat data have also been used in the monitoring of natural disasters [15]. Gombeer [16] has used Meteosat and GOES (Geostationary operational Environmental satellites) images of West Africa to compare the corresponding areas on the 1:5,000,000 FAO/UNESCO soil map. He concluded that the limits on the images which correspond fairly well to the limits of major soil units on the maps have been traced by using the gray tonality. The author also suggested potential applications for the Meteosat and GOES imageries based on broad synoptic character and the high repetition. These characteristics are important for studying the dust transports and deposits, moving dunes and forest advances or retreats [17].

Gombeer [16] stated that using Meteosat data and reports from synoptic weather and rainfall stations, algorithms were developed to map rainfall, net radiation, evapotranspiration, soil moisture availability, thermal inertia, and germinations. These algorithms were applied to a test area in Mali to map and monitor these variables during a test period of 18 days. The results demonstrated the ability of Meteosat to provide information in areas where ground stations are scarce or existing measurements unreliable.

Practically, Meteosat was used to study a thunderstorm case over the eastern desert cliffs, Qena area, Egypt on April 13 and 14, 1985. The thunderstorm occurred as a result of occasional monsoon low movement from the Sudan to the Gulf through Egypt as following sequence:

1. On April 11, 1985, instability of weather started in Qena area, related to the advancing of both the cold front coming from west and the Sudanese monsoon low from South (**Figure 9**).
2. On April 12, 1985, the Sudanese monsoon low continued to advance northwards and reached latitude 20, while the entire area was dry (**Figure 10**).
3. On April 13, 1985, the Sudanese monsoon low staked to a heavy cloud over the Qena area, which caused the thunderstorms. The dancing of the cold front from the west has helped in pushing the cloud toward the sea mountain and its ascending resulted in the flash rain (**Figure 11**).

This thunderstorm has caused the destruction of Khozam dam, which was built to protect the village of Khozam against the thunderstorm. It resulted also in lot of extreme damage in the village where the water reached a height of 2.25 m.

5. Evaluation of soil degradation in Northern Sinai (Egypt), using remote sensing and GIS

Soil degradation, as defined by FAO, UNEP [18] is “a process which lowers the current and/or the potential capability of soil to produce (quantitatively and/or qualitatively) goods or services.” In 1975, UNEP, FAO, and UNESCO develop a methodology for assessing soil degradation on a global scale. The methodology was tested in America north of the equator and in the near and Middle East.

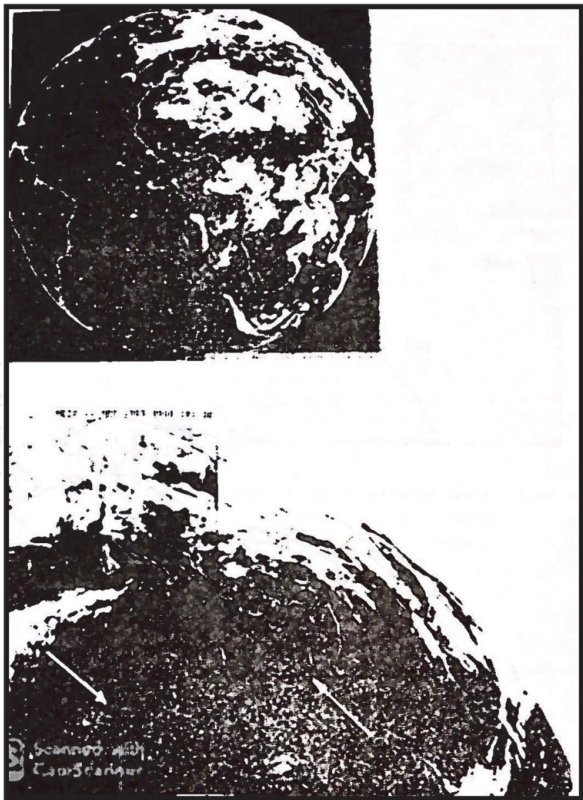


Figure 9.
Meteosat of April 11, 1985. It shows the advancing of the Sudanese Monsoon from the South toward the Red Sea. At the same time, the cold front started to move from the west the east.

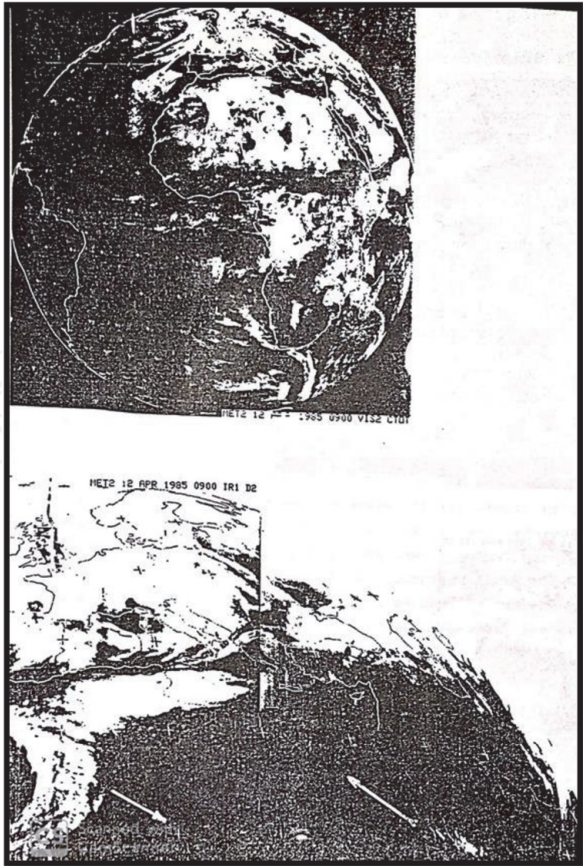


Figure 10.
Meteosat of April 12, 1985. It shows the continuous movement of the Sudanese Monsoon to the latitude of 20N, while the entire area was dry. The same time the cold front started to move from the west the east. Also continue moving eastwards.

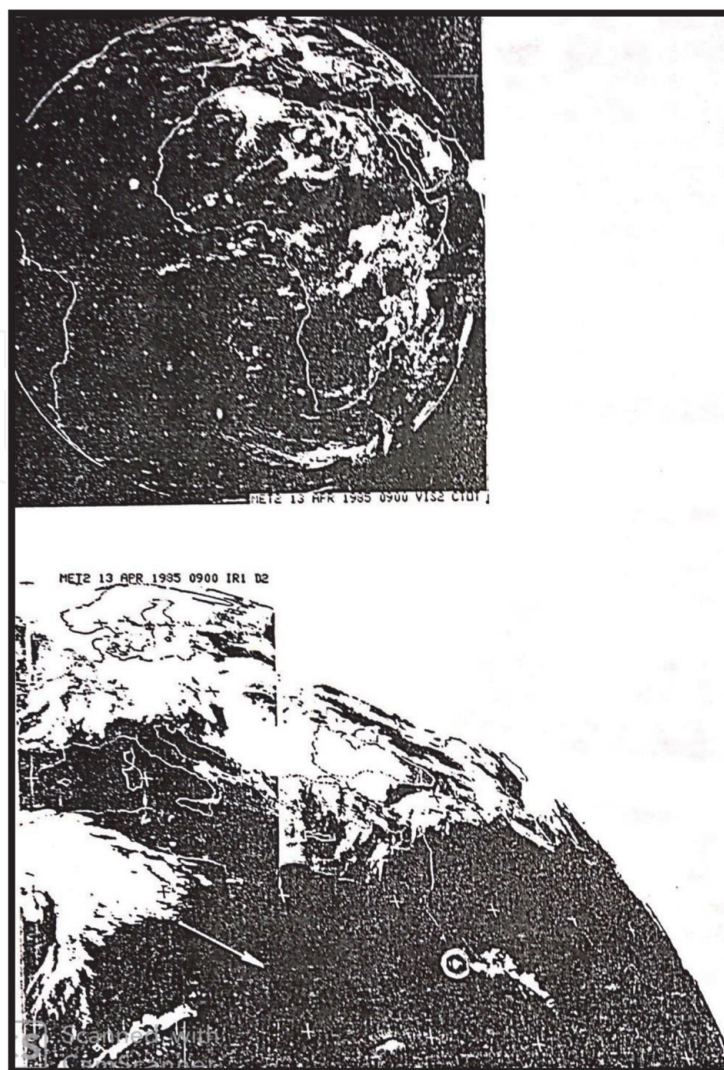


Figure 11.
Meteosat of April 13, 1985. The sticking of the Sudanese monsoon with clouds that caused the thunderstorms.

The recorded results are illustrated on four maps published at a 1:5,000,000 scale. It was clearly confirmed that soil degradation occurs over extended areas, which are not fully degraded then, but threatened by expected future degradation. Duly alienated by these results, FAO and UNEP [19] provided initiative to refine the original methodology to better serve scientists and managers in assessment of damage already done and future threats to land. The provisional methodology, published in 1983 has been developed to be scale independent, so that it may be applied at a global, national regional/provincial, and local project planning levels. It is designed to provide map able data that may potentially be used to plan strategies to conserve the remaining productive soil and to prevent soil degradation in areas not then affected.

The current study aims to assess soil degradation in north Sinai region, applying the above mentioned provisional methodology at 1:250,000 mapping scale. This scale is considered appropriate for planning at national level.

The Sinai Peninsula covers an area of 61,000 km², representing around 6% of Egypt's territories. It represents a promising and strategic region for economic development. Northern Sinai region has considerable potential for agriculture, fisheries, and summer resorts. Much of the arable land in this area would eventually be irrigated with Nile river water through the El-Salam canal [20]. The objectives of the study are to assess existing and potential risk of soil degradation. The following research aspect also highlights a remote sensing and GIS practitioner's viewpoint:

- To test soil degradation assessment methodology at 1:250,000 scale
- To use digital image processing and GIS techniques to derive input to the assessment model
- To evaluate the procedures and results

5.1 FAO concept of soil degradation monitoring and evaluation

Land degradation processes are phenomena that result in soil quality diminutions, leading to a risk of lowering current or potential productivities [21]. The present state of soil degradation is derived from the risk values by introducing the human activity represented by land use and soil management. Although often interacting, the soil degradation processes may be grouped into six categories, which are: water erosion, wind erosion, excess of salts, chemical degradation, physical degradation, and biological degradation. The current study assesses four of the six degradation processes, excluding only chemical and biological degradation. Soil degradation is expressed in the “FAO/UNRP and UNESCO provisional methodology” in units appropriate for each process. For example, soil erosion by water or wind is expressed by “soil loss in ton/ha/year” and salinization by “increase of EC in dS/m” and physical degradation by “increase of bulk density in g/cm³/year.” The degradation hazard values are then classified compared to listing of different soil degradation classes [22].

5.2 Assessment methodology and data sources

A parametric formula, based on the universal soil loss equation (USLE), was used [23]. Input data values are derived from a combination of direct measures and information of remote sensing and thematic maps. The formula can be expressed in the general form as:

$$D = .f(C, S, T, V, L, M)$$

where D is degradation, C is climatic aggressiveness factor, S is the soil factor, T is the topographic factor, V is the natural vegetation factor, L is the land use factor, and M is the management factor. For each degradation process, a similar formula is used. The values of the variables are chosen in such a way that solving of the equation gives a numeric indication of the degradation rate. The formula describes the processes only approximately and the values assigned to each factor are approximate in the present state of knowledge. Thus, the final results should not be regarded as absolute values for soil loss but as indication of the magnitude of degradation [24].

ArcGIS software is used to manage and manipulate the thematic map data, processed satellite images, and tabular data sources. ERDAS IMAGIN digital image processing programs are utilized to process the images, including radiometric and geometric correction, and to derive values of Normalized Difference of Vegetation Index (NDVI).

IDRISI software is employed with *ArcGIS* to generate slope values [25, 26].

5.3 Special processing concerns

Most of the data required the parametric formula were derived from map data sources or published data. The management factor or M value is derived from digitally processed satellite data.

The NDVI values are computed for each pixel in two 1024×104 datasets from 1984 Landsat MSS (**Figure 12**) and 1990 Landsat TM imagery (**Figure 13**). Iso-clustering classification is used to classify the NDVI images into six vegetation density classes. The classified images then converted to ArcGIS format and crossed with the soil coverage. The composed dataset is thus used in establishing a vegetation density rating for each soil polygon, thus deriving a management factor.

The other problem involves generating the percent slope data which are used in developing the rating of topography or (T factor) in the USLE. The following multi-step process is followed:

1. First, the digitizing of contour lines from 1:100,000 scale plan metric maps (**Figure 13**). *ArcGIS* line coverage is developed from digitized data and attributed with appropriate elevations.
2. Second, contour data are clipped to the digitized soil coverage and exported to IDRISI. A copy of the soil coverage is imported to IDRISI.
3. Third is the development of a digital elevation model (DEM) in IDRISI vector contour data.

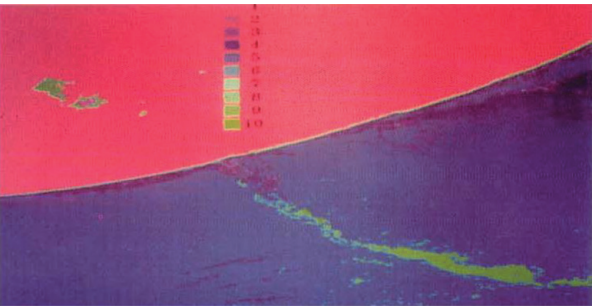


Figure 12.
Processed Landsat MSS—of Wadi El-Arish region, Sinai case study.

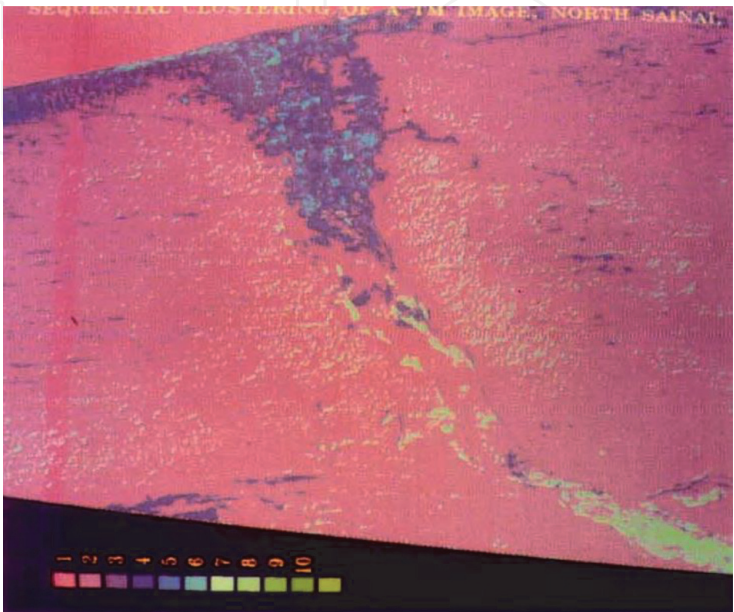


Figure 13.
Processed Landsat ETM—of Wadi El-Arish region, Sinai case study.

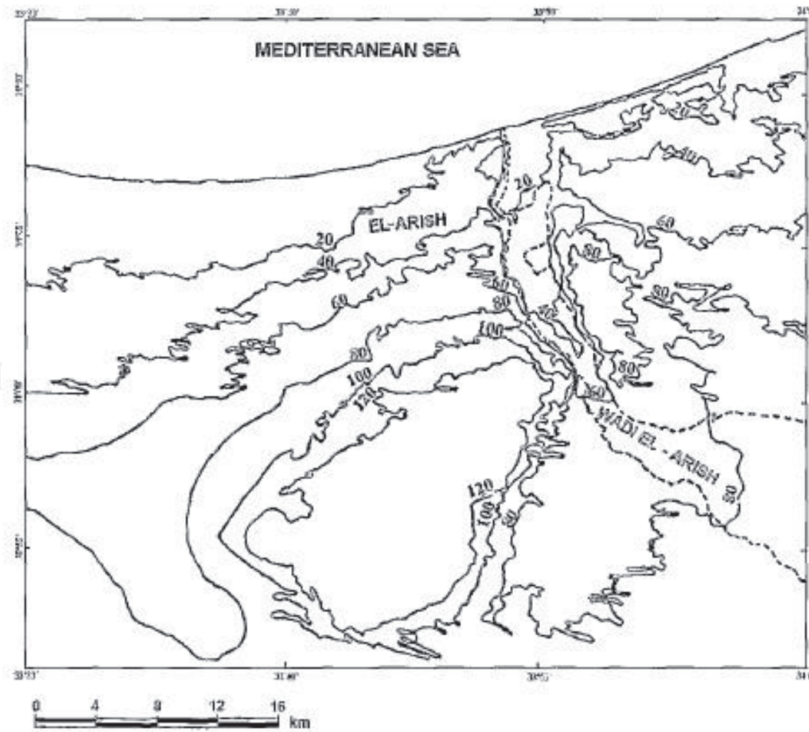


Figure 14.
Contour map of the Arish, Sinai study area.

4. Fourth, a percent slope value is generated for each cell.
5. Fifth step is to link a composite image of the percent slope data and the soil data.
6. Sixth and final step use the histogram to determine the distribution of slope values for each soil unit and to assign a percent slope class to each soil polygon.

5.4 Generation of the model

The soil coverage [20, 27] developed in ArcGIS is the base for generating the model (**Figure 14**). Climatic ratings, soil factors, topographic, vegetation, land use, and management ratings are added as attributes to the polygons of the soil coverage. Four soil profiles, representing different soil types in the study area, were investigated. Soil samples were collected and laboratory analyzed for calculating the soil factor acc. USLE. Computing the parametric equations is then completed for the four soil degradation processes, both for current soil degradation and the risk of soil degradation.

6. Results and discussions

Tables 1 and **2** show the laboratory analyses of the collected soil samples. Determination of the soil factor in the USLE is based on the results of these analyses. The soil erodibility factor for water erosion is calculated from Wischmeier's nomograph [28]. A correlation between soil texture and the wind erodibility was used [29]. Soil texture and depth to ground water have been utilized for rating the soil factor in salinization. The silt clay ratio is considered as an important factor contributing to the physical degradation process, as shown in **Figure 15** [24].

Profile no.	Depth (cm)	Mechanical analysis (mm)						Texture	O.M.	Structure
		2–>1	1–>0.5	0.5–>0.25	0.25–>0.125	0.125–>0.063	<0.063			
1	0–30	0	2	46.5	47.0	2	2.5	Sand	0.1	Loose
	30–60	0	1	50.0	46	2	1	Sand	nil	Loose
	60–100	0	5.5	58.0	33.5	2	1	Sand	nil	Loose
	100–150	0	10.5	58.5	25.5	1	1	Sand	Nil	Loose
2	0–40	0	1	11	82	3.5	2.5	Sand	0.1	Loose
	40–100	0	2.5	26.5	69	1	1	Sand	Nil	Loose
	100–150	0	7.5	18	72	1.5	1	Sand	Nil	Loose
3	0–35	0	3	10.1	35.1	22	9.8	S. loam	0.5	w. subang.
	35–70	0	1	2.90	50	27	17.5	S. loam	0.4	w. subang
	70–120	0	3.5	5.00	39.6	31.2	20.7	Loam	0.2	mod subang
4	0–60	0	2	39	48	7.5	5.5	Sand	0.4	Loose
	65–105	0	3	29.2	21.6	13.3	31.9	S. clay	–0.5	m.m. subang
	105–140	0	3.6	32.0	25.9	14.2	19.3	S. loam	0.3.	w.m. subang
	140–175	0	4.7	33.0	52.2	0	10.1	Sand	0.2	Loose

Table 1.
Some physical soil properties of selected soil profiles.

Profile no.	Depth	EC (mmohs/cm)	CaCO ₃ (%)	Soluble salts (mequiv./1)							
				Cations				Anions			
				Ca	Mg	Na	K	CO ₃	HCO ₃	Cl	SO ₄
1	0–30	0.5	6.3	1.7	0.9	2	0.5	0	0.8	2.8	1.5
	30–60	0.4	8.0	1.4	0.5	1.9	0.5	0	0.7	2.4	1.1
	60–100	0.5	10.1	2.1	0.3	1.9	0.4	0	0.7	2.5	1.5
	100–150	0.6	10.2	1.1	0.6	3.5	0.3	0	0.8	3.1	1.6
2	0–40	0.7	2	0.7	0.5	5.8	0.1	0	0.8	4.5	1.8
	40–100	0.8	0.3	0.6	0.4	7.5	0.2	0.5	0.9	6.1	1.2
	100–150	0.9	0.3	0.8	0.3	7.7	0.2	0.5	0.9	6.2	1.4
3	0–35	0.7	43.5	1.6	0.6	4.6	0.2	0	1.2	4.2	1.8
	35–70	1.1	54.5	1.8	1	7.9	0.2	0	1.3	5.8	3.8
	70–120	2.2	52.5	3.4	2.5	17	0.2	0	2.9	16.2	3.9
4	0–65	0.6	5.5	1.9	0.5	3.3	0.4	0	0.9	3.6	1.6
	65–105	2.5	28.5	2.6	2	21	0.2	0	3.1	18.4	4.4
	105–140	8.3	29.5	17	11.8	69	0.5	0	7.4	72	19.3
	140–175	6.1	23	12	8.9	50	0.4	0	7.4	43.8	19.8

Table 2.
Some soil chemical properties of selected soil profiles.

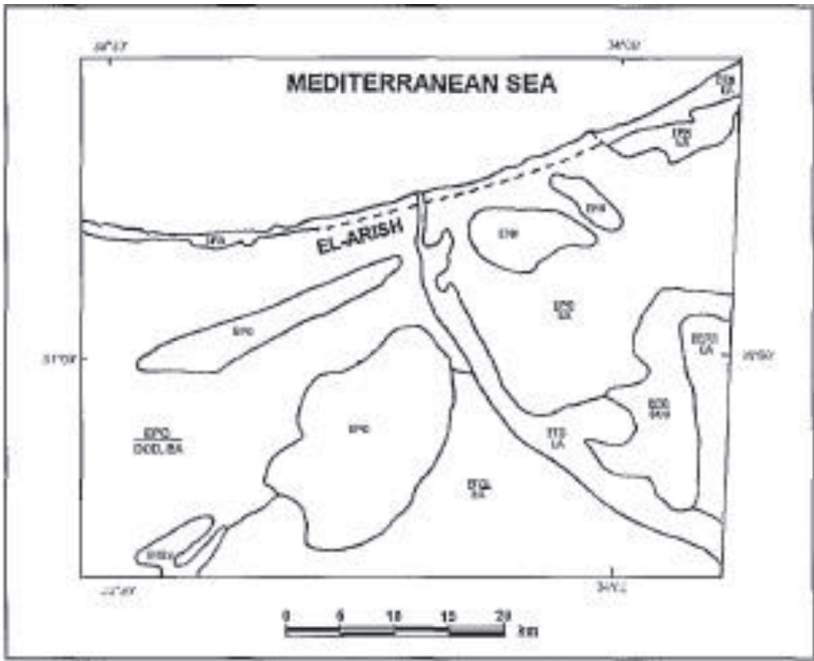


Figure 15.
Soil map of the Wadi El-Arish region, Sinai study area.

7. Water erosion

Table 3 shows the values of risk and present status of water erosion and the input parameters for their calculation. The area is generally exposed to a non to slight risk as the sand fraction is dominant in most soil types (**Table 1**). However,

Area (km ²)	ID	Soil type	Climatic factor	Soil factor	Topo. factor	Human factor	Risk	Present state
000051.130	1	EPA	16.39	0.03	0.35	0.32	0.1721	0.0551
000062.810	2	EPQ	16.39	0.03	2.00	0.45	0.9834	0.4425
000212.500	3	EPQ	16.39	0.03	2.00	0.45	0.9834	0.4425
000582.190	4	EPQ	16.39	0.03	2.00	0.45	0.9834	0.4425
000017.190	5	EHSS	16.39	0.08	0.35	0.07	0.4589	0.032 1
000301.875	6	EFCL/EA	16.39	0.08	0.35	0.07	0.4589	0.0321
000126.560	7	EFD/EA	16.39	0.08	0.35	0.07	0.4589	0.0321
000041.880	8	EPN	16.39	0.14	3.50	0.12	8.03 1	0.9637
							1	
000014.380	9	EPN	16.39	0.14	3.50	0.12	8.031	0.9637
							1	
000030.310	10	EPN/EA	16.39	0.14	3.50	0.12	8.0311	0.9637
000022.190	11	EPN/EA	16.39	0.14	3.50	0.12	8.03	0.9637
							11	
624514.990	12	EPQ/EA	16.39	0.03	2.00	0.45	0.9834	0.4425
000109.380	13	EPQ/ DOD	16.39	0.03	2.00	0.45	0.9835	0.4425
000053.750	14	EFGS/EA	16.39	0.08	0.35	0.07	0.4589	0.0321

Table 3.
Values of risk and present status of water erosion and the input parameters for their computation.

values of water erosion are the highest in the *Normipsammments* soils (EPN) as the topsoil is characterized by a sandy loam texture (soil profile no. 3) as opposed to the other soil units with sandy top soils.

8. Wind erosion

Table 4 shows the values of risk and present status of wind erosion and the input parameters for their calculation. Annual average of wind velocity, in El-Arish station reaches 4.30 Knots (2.214 m s^{-1}). Thus, the wind erosivity factor is high (50–150) in the study area. All soil types are characterized by high ($50\text{--}200\text{ t h}^{-1}\text{ year}^{-1}$) to very high ($>200\text{ t h}^{-1}\text{ year}^{-1}$) risk values of soil loss by wind erosion. Wind erosion in the study area is particularly important because the soils are mostly dry and the vegetation cover is scattered or absent. Cultivation of barley and non-conventional crops in some soils reduces the present state of wind erosion hazard. However, wind erosion is more pronounced in the *Psammments* soils (Quartzipsammments EPQ and *Aquipsammments* EPA), which are formed on sand dunes.

9. Salinization

Table 5 shows the values of risk and presents status of salinization and the input parameters for their calculation. The study area is characterized by hyper arid climatic conditions: the precipitation (P) is less than 1/3 of the potential evapo-transpiration (PET) and at least one 12 month period without rainfall. Thus, the proposed climatic index (PET/P) is very high (0.5–3.3).

The present state and risk values in the *Psammments* (i.e., EPA, EPQ, and EPN) are slight to moderate. The coarse texture and rapid permeability of these soils reduce

Area (km ²)	ID	Soil type	Climatic factor	Soil factor	Topo. factor	Human factor	Risk	Present state
000051.130	1	EPA	100	3.5	1	0.70	350	245.00
000062.810	2	EPQ	100	3.5	1	1.00	350	350.00
000212.500	3	EPQ	100	3.5	1	1.00	350	350.00
000582.190	4	EPQ	100	3.5	1	1.00	350	026.25
000017.190	5	EHSS	100	1.75	1	0.15	175	026.25
000301.875	6	EFCL/EA	100	1.75	1	0.15	175	026.25
000126.560	7	EFD/EA	100	1.75	1	0.15	175	052.50
000041.880	8	EPN	100	1.75	1	0.30	175	052.50
000014.380	9	EPN	100	1.75	1	0.30	175	052.50
000030.310	10	EPN/EA	100	1.75	1	0.30	175	052.50
000022.190	11	EPN/EA	100	1.75	1	0.30	175	052.50
624514.990	12	EPQ/EA	100	3.5	1	1.00	350	350.00
000109.380	13	EPQ/ DOD	100	3.5	1	1.00	350	350.00
000053.750	14	EFGS/EA	100	1.75	1	0.15	175	026.25

Table 4.
Values of wind erosion present status and risk and the input parameters for their computation.

Area (km ²)	ID	Soil type	Climatic factor	Soil factor	Topo. factor	Human factor	Risk	Present state
000051.130	1	EPA	1.50	0.1	1.0	0.7	0.150	0.105
000062.810	2	EPQ	1.50	0.1	1.0	0.5	0.150	0.075
000212.500	3	EPQ	1.50	0.1	1.0	0.5	0.150	0.075
000582.190	4	EPQ	1.50	0.1	1.0	0.5	0.150	0.075
000017.190	5	EHSS	1.50	1.0	5.0	0.7	7.500	5.250
000301.875	6	EFCL/EA	1.50	1.0	5.0	0.7	7.500	5.250
000126.560	7	EFD/EA	1.50	1.0	5.0	0.7	7.500	5.250
000041.880	8	EPN	1.50	1.0	0.1	0.7	0.150	0.105
000014.380	9	EPN	1.50	1.0	0.1	0.7	0.150	0.105
000030.310	10	EPN/EA	1.50	1.0	0.1	0.7	0.150	0.105
000022.190	11	EPN/EA	1.50	1.0	0.1	0.7	0.150	0.105
624514.990	12	EPQ/EA	1.50	0.1	1.0	0.5	0.150	0.075
000109.380	13	EPQ/ DOD	1.50	0.1	1.0	0.5	0.150	0.075
000053.750	14	EFGS/EA	1.50	1.0	5.0	0.7	7.500	5.250

Table 5.
Values of risk and present status of salinization and the input parameters for their computation.

the risk of salinization. *Haplorthents* (EHSS) and *Fluvents* (EFGS, EFD, and EFCL) are exposed to a very high risk of salinization. This is related to their shallow soil profiles, fine texture, and medium to low permeability. Since *Fluvents* occur in wadis, valley floors, desert basins, and playas, the topographic factor increases the salinization risk. Furthermore, agricultural practices on these soils, especially the excessive application of irrigation water, increase salinization hazard.

10. Conclusion and recommendation

Management and planning agricultural expansion in desert areas are essential for self-sufficiency of food production. However, many degradation processes, which are severe environmental extremes, are active on the soil and cause deterioration in their potential productivity. The evaluation and control of soil degradation and productivity are based on environmental information. GIS techniques are useful in storing, retrieving, and manipulating such information. Furthermore, remote sensing techniques GIS are useful in updating the status of soil deterioration and providing services to a risk model. It should be advised that the final values generated by parametric equations are not absolute values of soil loss. These values merely give an approximate indication of the likely magnitude of degradation. Additionally, better sources of data for the management factor and percent slope information need to be identified.

IntechOpen

IntechOpen


Author details

Abd-alla Gad

National Authority of Remote Sensing and Space Sciences (NARSS), Egypt

*Address all correspondence to: abdallagad1@gmail.com

IntechOpen

© 2020 The Author(s). Licensee IntechOpen. Distributed under the terms of the Creative Commons Attribution - NonCommercial 4.0 License (<https://creativecommons.org/licenses/by-nc/4.0/>), which permits use, distribution and reproduction for non-commercial purposes, provided the original is properly cited. 

References

- [1] Gómez F. Extreme environment. In: Gargaud M et al., editors. *Encyclopedia of Astrobiology*. Berlin, Heidelberg: Springer; 2011
- [2] Taminiau J, Nyangon J, Lewis AS, Byrne J. Sustainable business model innovation: Using polycentric and creative climate change governance. In: Fields Z, editor. *Collective Creativity for Responsible and Sustainable Business Practice*. IGI Global; 2017. pp. 140-159
- [3] UNCCD. Article 2 of the Text of the United Nations Convention to Combat Desertification. 1994. Available from: <http://www.unccd.int/Lists/SiteDocumentLibrary/conventionText/conv-eng.pdf>
- [4] Westin FC. Soil and land resource inventory using Landsat data. In: *Remote Sensing for Resource Management*. Ankeny, Iowa: Soil Conservation Society of America; 1982. pp. 243-254
- [5] Hill E. A deep crustal shear zone exposed in western Fiordland, New Zealand. *Tectonics*. 1995;**14**:1172-1181
- [6] FAO/UNEP and UNESCO. *A Provisional Methodology for Soil Degradation Assessment*. Rome: FAO; 1999
- [7] Miller JD, Hutchins M. The impacts of urbanisation and climate change on urban flooding and urban water quality: A review of the evidence concerning the United Kingdom. *Journal of Hydrology: Regional Studies*. 2017;**12**:345-362. DOI: 10.1016/j.ejrh.2017.06.006
- [8] Binns T. Is desertification a myth? *Geography*. 1990:106-113
- [9] Helldén U. Desertification: Time for an assessment? *Ambio*. 1991;**20**(8): 372-383
- [10] Hill J, Hostert P, Tsiourlis G, Kasapidis P, Udelhoven TH, Diemer C. Monitoring 20 years of increased grazing impact on the Greek island of Crete with earth observation satellites. *Journal of Arid Environment*. 1998;**39**: 165-178
- [11] Thomas DSG, Middleton NJ. *Desertification: Exploding the Myth*. Chichester: Wiley; 1994
- [12] Barrett EC, Hamilton MG. The use of geostationary satellite data in environmental science. *Progress in Physical Geography*. 1982;**6**(2):159-214
- [13] Darnll WI, Harris RC. Satellite surface capability for surface temperature and meteorological parameters over the oceans. *International Journal of Remote Sensing*. 1983:65-92. 1pp
- [14] Eigenwillig N, Fischer H. Determination of midtropospheric wind vectors by tracking pure water vapor structures in METEOSAT water vapor image sequences. *Bulletin of the American Meteorological Society*. 1982; **63**:44-58
- [15] Robson A, Morgan J, Herschy RW, Zchav J. Detection of natural disasters via Meteosat. *ESA Bulletin*. 1982;**29**: 10-18
- [16] Gombeer R. Crop and land use classification study on SAR and MSS data over Belgium ESA SAR 580 Invest. Preliminary Report. 1983
- [17] Nicholson S, Jinnah S, Gillespie A. Solar radiation management: A proposal for immediate polycentric governance. *Climate Policy*. 2018;**18**(3):322-334. DOI: 10.1080/14693062.2017.1400944
- [18] FAO/UNEP. *Guidelines for the Control of Soil Degradation*. Rome, Italy: FAO; 1983

- [19] FAO/UNEP. Report on the FAO \UNEP expert consultation on methodology for assessing soil degradation. In: Project no. 1106-75-05. Rome, Italy: FAO; 1978
- [20] Hammami M. Land master plan region report—Sinai, Cairo, Ministry of Development, General Authority for Rehabilitation Project and Agricultural Development. 1986
- [21] Lal R, Stewart A. Soil Degradation. New York: Springer-Verlag; 1990
- [22] FAO/JNEP, UNESCO. A Provisional Methodology for Soil Degradation Assessment. Rome, Italy: FAO; 1979
- [23] Soil Science Society of America (SSSA). Universal soil loss equation: Past, present and future. In: SSSA Special Publication Number 8. Madison, Wisconsin: SSSA; 1979
- [24] Shalaby A, Ali RR, Gad A. AGIS-based model for desertification sensitivity assessment, case study: Inland Sinai and Eastern Desert Wadies. International Journal of Basic and Applied Sciences. 2011;1(1):1-11
- [25] Gad A. Study of soil degradation processes in the eastern Nile Delta using GIS and Remote sensing. Egyptian Journal of Remote Sensing. 1993;1
- [26] Gad A, Younes, Abdel-Hadmy A. Assessment of soil degradation processes in the middle part of the Nile Valley, Egypt, using GIS and remote sensing techniques. In: Proceedings of the 15th World Congress of Soil Science, Acapulco, Mexico, 10-16 July. 1994. pp. 217-218
- [27] Abdel-Samae G, Labibt M, Abdel-Hady MA. Soil classification and potentials in Sinai peninsula from Landsat images. In: Proceedings of the International Symposium on Remote Sensing in Arid and Semi-arid Lands; Cairo, Egypt, January. 1982
- [28] Kim JH, Keane TD, Bernard EA. Fragmented local governance and water resource management outcomes. Journal of Environmental Management. 2015;150:378-386
- [29] Kimberlin LW, Hidlebaugh L, Grimewald R. The potential wind erosion problem in the United States. Transactions of ASAE. 1977